# Arrhythmogenic right ventricular cardiomyopathy: Electroarchitecture of the substrate

Atsuyuki Watanabe, MD,[*] Atsuko Seki, MD,[†] Michael C. Fishbein, MD,[†] Kalyanam Shivkumar, MD, PhD, FHRS,[*] Marmar Vaseghi, MD, MS, FHRS[*]

*From the [*]UCLA Cardiac Arrhythmia Center, and [†]Department of Pathology and Laboratory Medicine, University of California, Los Angeles, California.*

## Introduction

Arrhythmogenic right ventricular cardiomyopathy (ARVC) is characterized by ventricular arrhythmias and fibrofatty replacement of the right ventricular (RV) myocardium. Although the RV is the predominant chamber involved, left ventricular (LV) involvement has also been documented.[1–4] Electrophysiological correlations of histopathologic findings in nonischemic cardiomyopathy, and especially in ARVC, are limited.[5] We report a case of ARVC that presented with ventricular tachycardia (VT) and diffuse fibrofatty involvement of both the RV and LV. A detailed analysis of the electrophysiological, cardiac imaging, and pathologic findings was performed, providing insights into the electroachitecture of the myocardium and electrical manifestations of the pathologic findings.

## Case report

A 57-year-old female with a family history of ventricular arrhythmias and ARVC was implanted with a dual-chamber implantable cardioverter defibrillator. Because of recurrent VTs and defibrillator shocks, she underwent electrophysiological study and epicardial and endocardial catheter ablation of the VT in September 2011. A total of 2815 epicardial and 1110 endocardial voltage points were obtained. The epicardial electroanatomic map demonstrated extensive scarring of the RV free wall and LV anterior wall. The endocardial map showed extensive scarring of the interventricular septum (IVS) and right ventricular outflow tract (RVOT). Late potentials, particularly on the RV anterior free wall, were noted on the epicardium. A slow monomorphic VT (left bundle branch block configuration and inferior axis, cycle length 580 to 750 milliseconds) was induced (Figure 1) and terminated during ablation in the RVOT. Rather than targeting the extensive low-voltage areas identified as "scar" on both the LV and RV by electroanatomic mapping, specific sites with late potential and late fractionated electrograms (EGMs) were targeted, particularly on the epicardial and endocardial aspect of the RVOT. The patient underwent orthotopic heart transplantation in September of 2014 for progressive heart failure. Ex vivo cardiac magnetic resonance imaging (MRI) was performed on the explanted heart along with a comparative investigation of the electrophysiological, pathologic, and imaging findings. The explanted heart demonstrated marked infiltration of fibrofatty tissue, with areas of complete transmural myocardial replacement. The pathological findings correlated well with cardiac MRI results, but MRI could not distinguish between epicardial fat and fibrofatty replacement of the LV (Figure 1). EGMs from multiple regions with very low voltage (<0.5 mV) and border zones (0.5 to 1.5 mV), as well as viable myocardium on EAM were analyzed and the histologic findings at these sites evaluated (Figures 2 and 3). The patient remained arrhythmia free postablation and underwent heart transplantation for heart failure.

## Discussion

ARVC is characterized by RV myocyte loss and fibrofatty tissue replacement, and it predisposes patients to life-threatening ventricular arrhythmias.[6] Biventricular and left-dominant forms of the disease, although less common, are increasingly recognized.[1–4] In this case, the patient had experienced multiple episodes of syncope and had shown evidence of RV dilatation on an echocardiogram as early as 1993 in her native country, but she was not diagnosed till 2009, when she presented with syncope from VT, family history of ARVC, RV dilatation on echocardiogram, and presence of epsilon waves on electrocardiograms. At the time of transplantation, notably thick, diffuse fibrofatty tissue infiltration of both the RV and LV was observed. The degree of infiltration was so extensive that, on in vivo MRI

**KEYWORDS** Arrhythmogenic right ventricular cardiomyopathy; Cardiac MRI; Catheter ablation; Pathology; Ventricular tachycardia

**ABBREVIATIONS** **ARVC** = arrhythmogenic right ventricular cardiomyopathy; **EAM** = electroanatomic mapping; **EGM** = electrogram; **IVS** = interventricular septum; **LV** = left ventricle; **MRI** = magnetic resonance imaging; **RV** = right ventricle; **RVOT** = right ventricular outflow tract; **VT** = ventricular tachycardia

(Heart Rhythm Case Reports 2016;2:47–51)

**Address reprint requests and correspondence:** Dr Marmar Vaseghi, UCLA Cardiac Arrhythmia Center, 100 Medical Plaza, Suite 660, Los Angeles, CA 90095. E-mail address: mvaseghi@mednet.ucla.edu.



http://dx.doi.org/10.1016/j.hrcr.2015.09.004

## KEY TEACHING POINTS

- Local abnormal ventricular activities and late potentials on electroanatomic mappings correlate with inhomogeneous areas of surviving myocardium admixed with fibrofatty tissue on histopathology. Only fat was observed in areas denoted by low-voltage (<0.5 mV), short-duration electrograms on the electroanatomic map.
- The site of successful ablation of ventricular tachycardia was in very close proximity to a heterogenous substrate consisting of surviving myocardium and fibrofatty tissue on histopathology.
- This case of arrhythmogenic right ventricular cardiomyopathy demonstrated diffuse thick fibrofatty infiltration of both ventricles, including the interventricular septum, with irregular areas of fibrofatty tissue noted in most of these regions.

results, it was difficult to distinguish between myocardial fibrofatty infiltration and epicardial fat. The fibrofatty tissue covering the LV had the same thickness as the viable LV myocardium, and the entire RV myocardium had been replaced. Further, fibrofatty infiltration into the IVS was demonstrated on MRI and histologic findings (Figure 1).

The findings on histopathology closely matched those of MRI performed ex vivo (Figure1C), supporting the notion that MRI remains an important tool for evaluating fibrofatty infiltration in patients with ARVC before electrophysiological study.[7,8] Although this patient did not undergo heart transplantation immediately after VT ablation, the EAM and histopathology findings correlated well, as suggested by a recent study showing that the majority of ARVC patients have similar electroanatomic maps at mean of 57 months apart.[9] Of note, the fibrofatty infiltration in this case was not homogenous. In addition to "linear" fibrofatty layers in the IVS (Figure 1), very localized rounded infiltrations in the LV anteroapex (Figure 2) and infiltrating layers in the RVOT (Figure 3) were observed. This heterogeneous infiltration, or tissue anisotropy, has important implications for arrhythmogenesis, serving as the substrate for arrhythmias and sites of reentry.

It has been previously reported that the presence of epicardial fat can confound quantification of electrophysiological scar on EAM, as both myocardial fibrosis and fat are

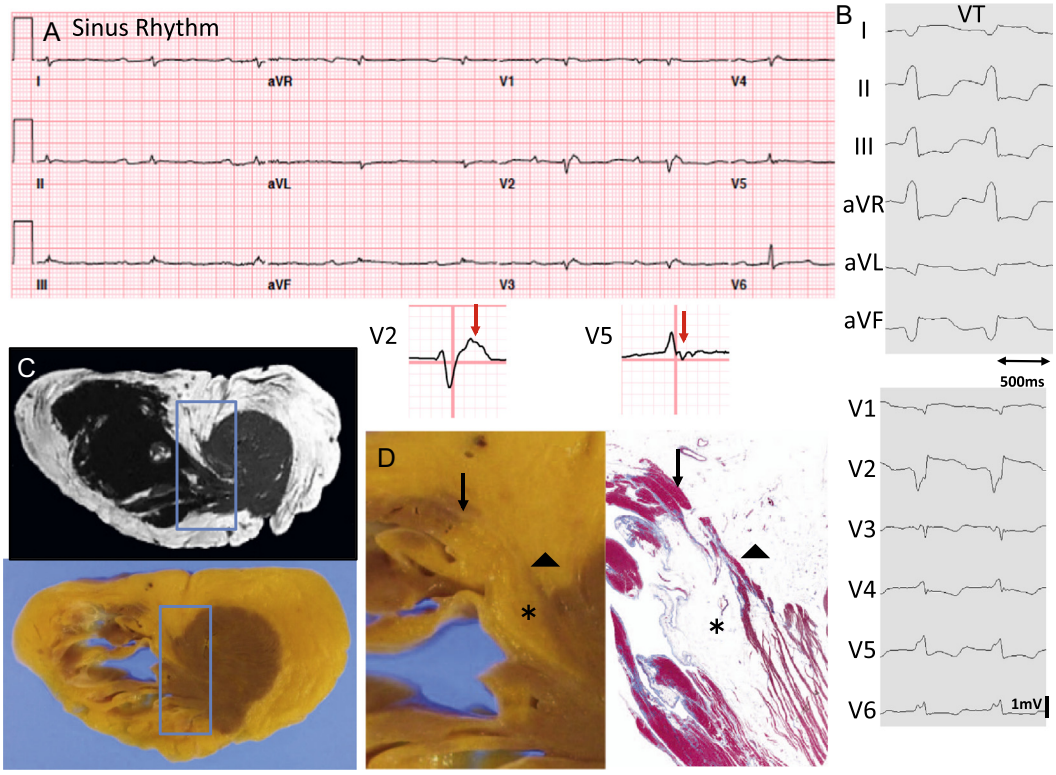


**Figure 1** **A:** A 12-lead electrocardiogram showing sinus rhythm. The electrocardiogram in sinus rhythm demonstrates epsilon waves in V1-V5 (red arrow), and low voltage, given epicardial-to-endocardial fibrofatty infiltration. **B:** Ventricular tachycardia morphology observed during electrophysiological study is consistent with a right ventricular outflow tract origin. **C:** Comparison of ex vivo cardiac magnetic resonance image (left upper panel) and gross pathologic section (left lower panel). Thick diffuse fatty tissue around the right ventricle and left ventricle was observed. There is evidence of fibrofatty infiltration in both ventricles, including in the interventricular septum (IVS) (blue square). **D:** Fatty infiltration in the IVS on the gross (left panel) and histopathologic (right panel) sections demonstrates an area with surviving myocardium surrounded by fibrofatty infiltration. (Asterisk, arrow, and arrowhead point to similar regions between the gross and histopathologic sections.)

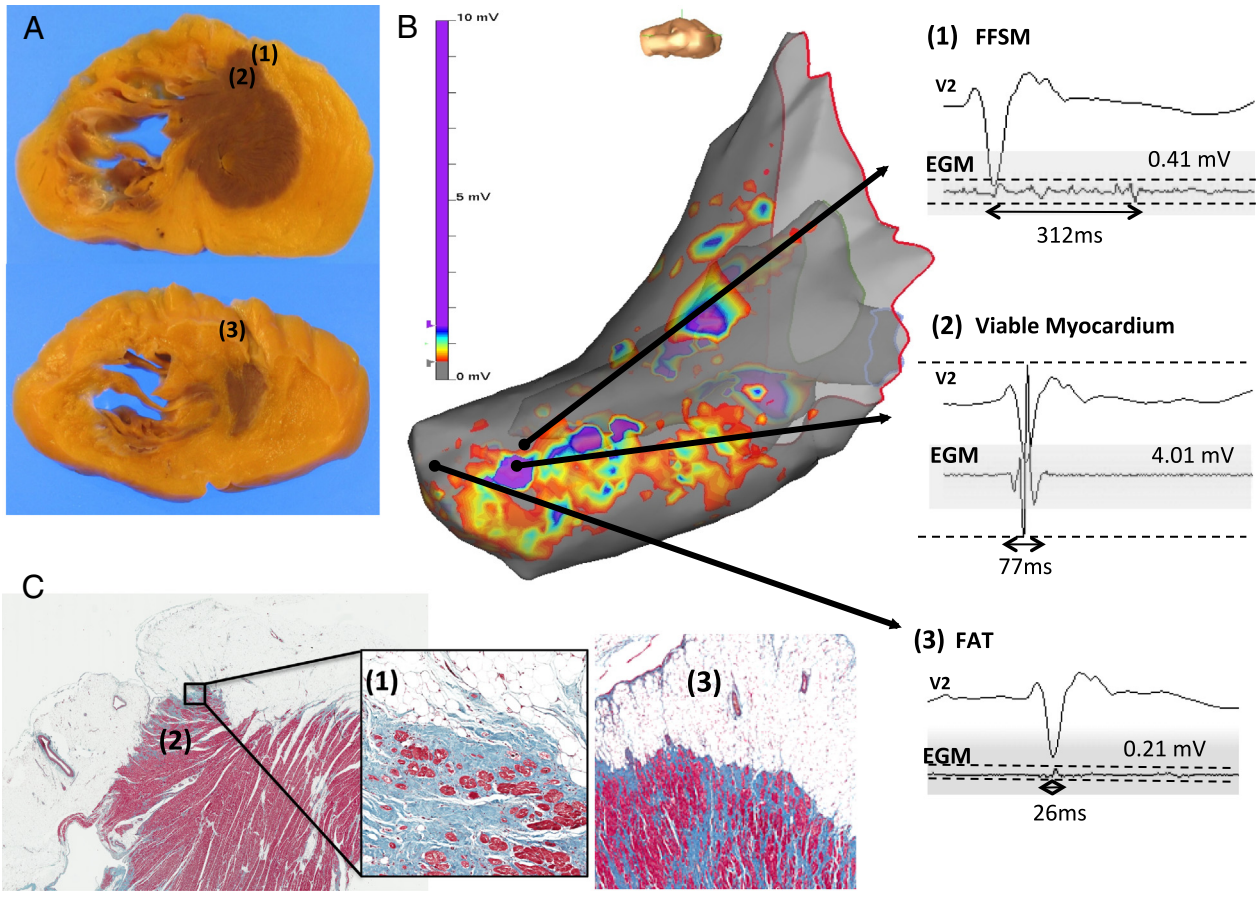


**Figure 2** Correlation of electroanatomic mapping with gross pathology **A:** A gross section of the left ventricle (LV) demonstrates surviving myocardium in the LV anteroapex (upper panel) and apex covered with fibrofatty tissue (lower panel). **B:** Superimposed right ventricular (RV) endocardial and epicardial electroanatomic mappings (EAMs). The electrograms (EGMs) from corresponding sites in panel A are shown. A fractionated EGM with evidence of a late potential is observed in the border-zone region between surviving myocardium and fat. The surviving myocardium shows normal voltage, while fat demonstrates very low-voltage EGMs. **C:** Histopathologic findings from the gross section shown in panel A and the corresponding sites on EAMs and EGMs from panel B are shown: (1) Significant fibrofatty infiltration with surviving myocardium (FFSM) was seen in an area of fractionated EGM with late potentials; (2) predominantly viable myocardium with some interstitial fibrosis was seen in an area of normal voltage; and (3) epicardial fat was seen in an area of low-voltage, short-duration EGM.

represented by low-voltage signals.[8,10–12] In animal models, surviving islands of myocardium within scars of healed myocardial infarcts exhibit more fractionation and longer duration EGMs compared to fatty tissue overlying normal myocardium.[12] In this case, extensive low-voltage areas were observed on the ventricular epicardium on EAM (Figures 2 and 3), but based on but on histopathology, represented predominantly fat. Fractionation and late potentials were observed in the RVOT and LV anteroapex locally (Figures 2 and 3). On histopathologic examination, in areas close to these ablation sites, a heterogeneous substrate consisting of fibrofatty tissue and surviving myocytes was seen. Ablation from both the epicardium and endocardium in these regions created areas of transmural fibrosis (Figure 3), ranging from 600 μm to 1.5 mm in depth, including in the region of VT termination, Surviving islands of myocardium within the fibrofatty tissue served as the substrate for VT, whereas low-voltage areas without late potentials or fractionation were not important targets for ablation. In this patient, given the presence of histopathologic confirmation, we analyzed the voltage and duration of 25 EGMs from areas of pure fibrofatty tissue (FFSM), fibrofatty infiltration with surviving myocardium, and viable myocardial regions without fibrosis or fat (Figure 3C). Areas of thick fibrofatty infiltration with little viable myocardium exhibited low-voltage and short-duration EGMs (voltage 0.17 ± 0.14mV, duration 59 ± 20 milliseconds, mean ± SD). On histopathology areas of surviving myocardium admixed with fibrofatty tissue, exhibited low-voltage and long-duration EGMs (voltage 0.30 ± 0.12mV, duration 109 ± 28 milliseconds, mean ± SD), and border-zone regions with surviving myocytes exhibited long-duration EGMs (voltage 0.89 ± 0.39 mV, duration 89 ± 31 milliseconds, mean +/- SD). Normal myocardium demonstrated high-voltage, short-duration EGMs (voltage 2.78 ± 1.47 mV, duration 69 ± 16 milliseconds). These findings confirm that islands of surviving myocardium within fibrofatty tissue of ARVC, similar to myocardia infarcts, are electrically active and represented by low-voltage, long-duration EGMs.

Percutaneous epicardial mapping has become an important strategy for ablation of VT in ARVC cases.[13–15] Rather

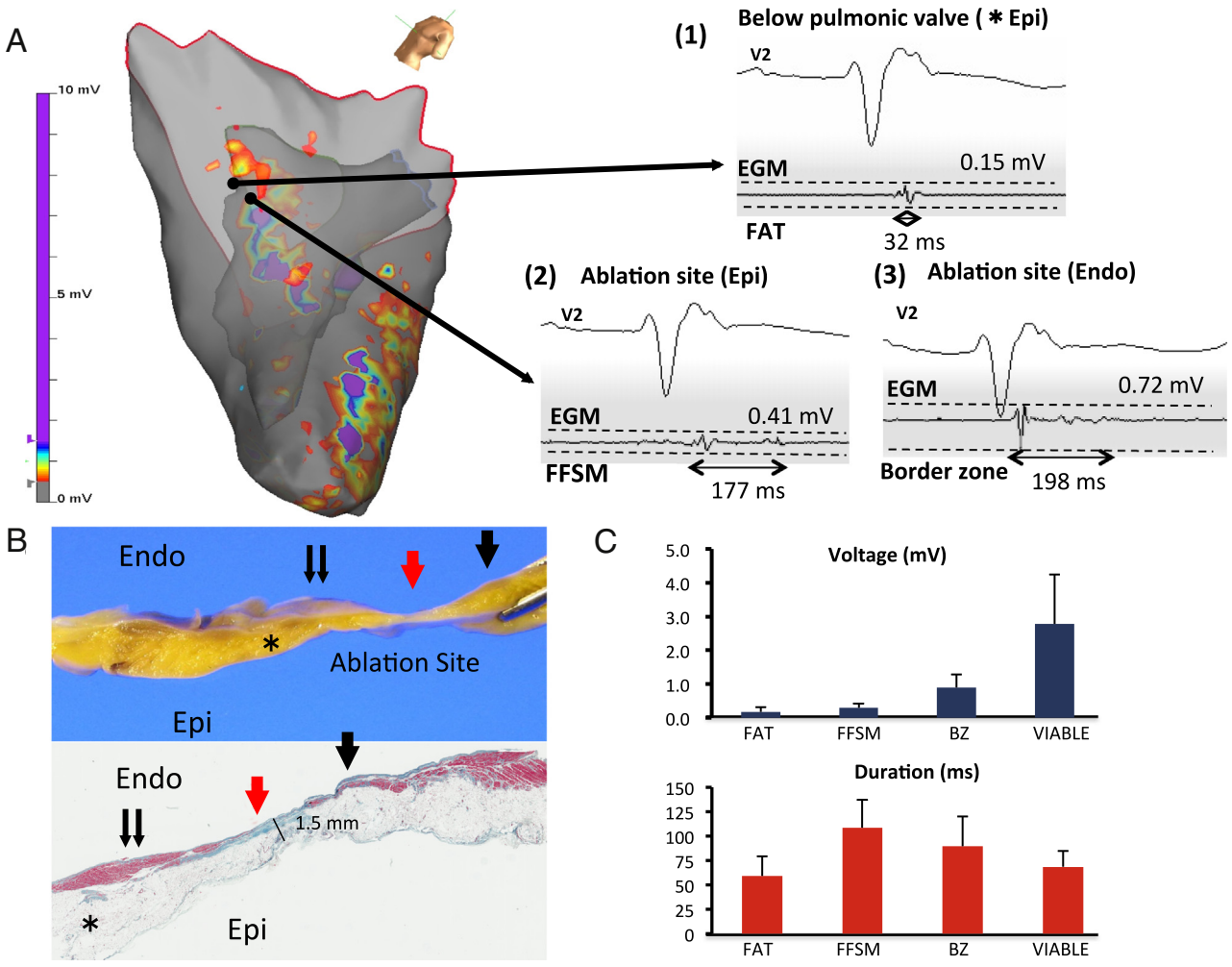


**Figure 3** Correlation of electroanatomic mapping with histopathologic findings in the right ventricular outflow tract (RVOT). **A**: Electrograms (EGMs) from an area of low voltage below the pulmonic valve and 2 sites on the epicardium (Epi) and endocardium (Endo) prior to ablation are shown. **B:** Gross section (upper panel) and corresponding histopathologic findings (lower panel) of an ablated region in the RVOT. The red arrow points to the ablation site, and the black arrows demonstrate corresponding sites between gross and histologic sections. The corresponding EGMs in panel A from both epicardium and endocardium (red arrow) prior to ablation demonstrate fractionation and late potentials. After ablation, this site shows a transmural fibrotic lesion. The asterisk demonstrates fat below the pulmonic valve on histologic findings (region 1). **C:** Analysis of a total of 100 EGMs (25 from each region) of corresponding sites on histologic findings and electroanatomic mappings (EAMs). Pure fatty or fibrofatty replacement had low-voltage, short-duration EGMs. Sites near areas of normal voltage consisting of surviving myocardium surrounded by fibrofatty infiltrations exhibited low-voltage but long-duration EGMs. Areas with border-zone EGMs (voltage between 0.5 and 1.5 mV) often also contained fatty or fibrofatty infiltration with surviving islands of myocardium and exhibited EGMs of long duration. FFSM = fibrofatty infiltration admixed with surviving myocardium; BZ = border zones; FAT = fatty tissue without surviving myocytes; viable = areas of normal myocardium.

than targeting all low-voltage areas, which are extensive and likely represent fat, it is important to target fractionated and late potential EGMs of long duration that represent areas of surviving myocardium within fibrous tissue.

## Conclusion

This case report sheds light upon the electrical manifestations that serve as the histopathologic signature of arrhythmias in ARVC, in addition to emphasizing important limitations faced in ablation of these cases, such as thickness of fatty tissue and infiltration into the IVS. It confirms that islands of surviving myocardium admixed with fibrofatty tissue of ARVC are electrically active; create tissue anisotropy; are represented by low-voltage, long-duration EGMs; and serve as the substrate for VT.

## Acknowledgments

This study was supported by grants from the American Heart Association (AHA 11FTF75500) to Marmar Vaseghi and the National Institute of Health (NHLBI RO1 HL084261) to Kalyanam Shivkumar.

## References

1. Gallo P, d'Amati G, Pelliccia F. Pathologic evidence of extensive left ventricular involvement in arrhythmogenic right ventricular cardiomyopathy. Hum Pathol 1992;23:948–952.
2. Sen-Chowdhry S, Syrris P, Prasad SK, Hughes SE, Merrifield R, Ward D, Pennell DJ, McKenna WJ. Left-dominant arrhythmogenic cardiomyopathy: An under-recognized clinical entity. J Am Coll Cardiol 2008;52:2175–2187.
3. Protonotarios A, Patrianakos A, Spanoudaki E, Kochiadakis G, Michalodimitrakis E, Vardas P. Left dominant arrhythmogenic cardiomyopathy: A morbid association of ventricular arrhythmias and unexplained infero-lateral T-wave inversion. J Electrocardiol 2013;46:352–355.

4. Marchlinski FE, Zado E, Dixit S, Gerstenfeld E, Callans DJ, Hsia H, Lin D, Nayak H, Russo A, Pulliam W. Electroanatomic substrate and outcome of catheter ablative therapy for ventricular tachycardia in setting of right ventricular cardiomyopathy. Circulation 2004;110:2293–2298.
5. Cesario DA, Vaseghi M, Boyle NG, Fishbein MC, Valderrábano M, Narasimhan C, Wiener I, Shivkumar K. Value of high-density endocardial and epicardial mapping for catheter ablation of hemodynamically unstable ventricular tachycardia. Heart Rhythm 2006;3:1–10.
6. Tscharbrunn C, Marchlinski FE. Ventricular tachycardia mapping and ablation in arrhythmogenic cardiomyopathy/dysplasia: lessons learned. World J Cardiol 2014;6:959–967.
7. Sen-Chowdhry S, McKenna WJ. The utility of magnetic resonance imaging in the evaluation of arrhythmogenic right ventricular cardiomyopathy. Curr Opin Cardiol 2008;23:38–45.
8. Piers SR, van Huls van Taxis CF, Tao Q, van der Geest RJ, Askar SF, Siebelink HM, Schalij MJ, Zeppenfeld K. Epicardial substrate mapping for ventricular tachycardia ablation in patients with non-ischaemic cardiomyopathy: A new algorithm to differentiate between scar and viable myocardium developed by simultaneous integration of computed tomography and contrast-enhanced magnetic resonance imaging. Eur Heart J 2013;34:586–596.
9. Riley MP, Zado E, Bala R, et al. Lack of uniform progression of endocardial scar in patients with arrhythmogenic right ventricular dysplasia/cardiomyopathy and ventricular tachycardia. Circ Arrhythm Electrophysiol 2010;3:332–338.
10. Nakahara S, Tung R, Ramirez RJ, Michowitz Y, Vaseghi M, Buch E, Gima J, Wiener I, Mahajan A, Boyle NG, Shivkumar K. Characterization of the arrhythmogenic substrate in ischemic and nonischemic cardiomyopathy implications for catheter ablation of hemodynamically unstable ventricular tachycardia. J Am Coll Cardiol 2010;55:2355–2365.
11. van Huls van Taxis CF, Wijnmaalen AP, Piers SR, van der Geest RJ, Schalij MJ, Zeppenfeld K. Real-time integration of MDCT-derived coronary anatomy and epicardial fat: Impact on epicardial electroanatomic mapping and ablation for ventricular arrhythmias. J Am Coll Cardiol Img 2013;6:42–52.
12. Tung R, Nakahara S, Ramirez R, Lai C, Fishbein MC, Shivkumar K. Distinguishing epicardial fat from scar: Analysis of electrograms using high-density electroanatomic mapping in a novel porcine infarct model. Heart Rhythm 2010;7:389–395.
13. Philips B, te Riele AS, Sawant A, Kareddy V, James CA, Murray B, Tichnell C, Kassamali B, Nazarian S, Judge DP, Calkins H, Tandri H. Outcomes and ventricular tachycardia recurrence characteristics after epicardial ablation of ventricular tachycardia in arrhythmogenic right ventricular dysplasia/cardiomyopathy. Heart Rhythm 2015;12:716–725.
14. Komatsu Y, Daly M, Sacher F, et al. Endocardial ablation to eliminate epicardial arrhythmia substrate in scar-related ventricular tachycardia. J Am Coll Cardiol 2014;63:1416–1426.
15. Bai R, Di Biase L, Shivkumar K, et al. Ablation of ventricular arrhythmia in arrhythmogenic right ventricular dysplasia/cardiomyopathy: Arrhythmia-free survival after endo-epicardial substrate based mapping and ablation. Circ Arrhythm Electrophysiol 2011;4:478–485.